

EFFECT OF PRESSURE ON PHONON MODES IN WURTZITE ZINC OXIDE

F. J. MANJÓN^{a,b,*}, K. SYASSEN^a and R. LAUCK^a

^aMax-Planck-Institut für Festkörperforschung, Heisenbergstr. 1, D-70569 Stuttgart, Germany; ^bDpto. de Física Aplicada, Universitat Politècnica de València, E.P.S.A. ES-03801 Alcoy, Spain

(Received 17 September 2001; In final form 17 October 2001)

The pressure dependence of first- and second-order Raman frequencies of wurtzite ZnO has been measured up to the wurtzite-rocksalt phase transition pressure of 8.3 GPa. A small increase of the LO-TO splitting with increasing pressure is observed. This effect is related to the combined pressure dependences of the electronic dielectric constant in the phonon region and Born's transverse dynamic effective charge. Our results indicate a rather weak dependence of the dynamic charge on pressure, a behavior which is similar to that found for GaN, AlN, and SiC and different from that of other polar tetrahedral semiconductors.

Keywords: Zinc oxide; II–VI semiconductors; Raman scattering; High pressure

PACS numbers: 62.50.+p, 78.30.Fs

INTRODUCTION

Zinc oxide at ambient conditions is a wurtzite-type semiconductor with a fundamental band gap of 3.4 eV. It is an important material in various fields of applications [1]. Unintentionally doped ZnO is *n*-type and usually exhibits a large free electron concentration which leads to a strong modification of the longitudinal-optic (LO) Raman scattering due to plasmon–phonon coupling, as occurs in other highly-doped polar semiconductors [2]. As a result, uncoupled LO Raman modes of ZnO are difficult to observe [3]. Raman measurements of wurtzite ZnO at ambient pressure have been reported by a number of groups [4–6]. High-pressure Raman studies of ZnO have been performed up to the phase transition for unspecified [7] and highly-doped sintered material [8] and, up to 1 GPa, for unintentionally-doped bulk crystals [9].

In this work we report results of a Raman study of unintentionally-doped ZnO measured at room temperature and under hydrostatic pressures up to ~ 11.5 GPa. We were mainly interested in the pressure dependence of the LO-TO mode splitting in ZnO, which provides information on the change of Born's transverse dynamic effective charge e_T^* of the lattice ions [10, 11]. Our experiments cover the stability range of the wurtzite modification which undergoes a transition to a rocksalt phase at pressures around 8–10 GPa (see, e.g., Refs. [12–16]).

* Corresponding author. Tel.: +34 96 652 84 42; Fax: +34 96 652 84 09; E-mail: fmanjon@fis.upv.es

EXPERIMENTAL PROCEDURE

After sublimation and oxidation of zinc (99.9995%), the ZnO crystals were grown by chemical vapour transport in a silica ampoule using ammonium chloride as a transport agent. A platelet-shape crystal ($100 \times 100 \mu\text{m}^2$ in lateral size and thickness less than $30 \mu\text{m}$) was fitted into a diamond anvil cell. A 4:1 methanol–ethanol mixture served as pressure medium and the ruby luminescence method was used for pressure calibration [17]. Raman experiments were performed in backscattering geometry using the 457.9 nm line of an Ar^+ -ion laser at power levels below 30 mW. The *c*-axis of the sample was oriented along the DAC axis. The scattered light was analysed by a Jobin-Yvon T64000 triple spectrometer using a CCD detector.

RESULTS AND DISCUSSION

Figure 1 shows selected Raman spectra of wurtzite ZnO measured for a first upstroke to 11.5 GPa, a downstroke to ambient pressure, and a second upstroke to 8.1 GPa. At pressures above 8.3(2) GPa (for both the first and second upstroke) the sample transformed to the rock-salt phase as indicated by the disappearance of the wurtzite Raman modes. Only broad features of rather low intensity are seen in all spectra measured above 8.3 GPa (not shown in Fig. 1). On decreasing pressure from 11.5 GPa, wurtzite-phase Raman modes of ZnO appeared again below 4 GPa. Thus, our room-temperature Raman data indicate the completion of the wurtzite to rocksalt transition near 8.3 GPa and a hysteresis of about 4 GPa for the

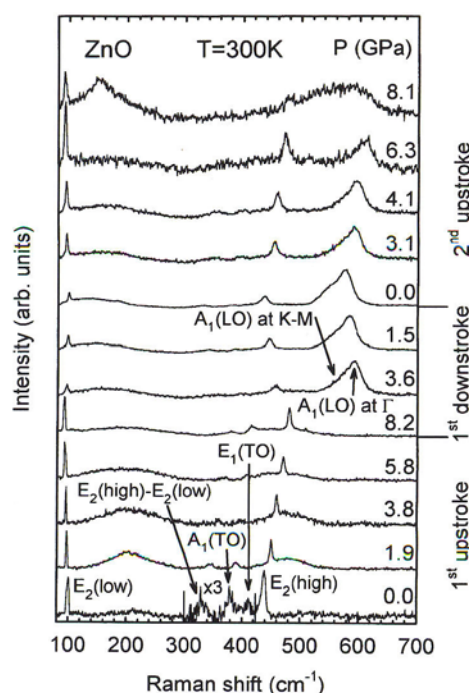


FIGURE 1 Raman spectra of ZnO as a function of pressure. Spectra were measured during a first upstroke to 11.5 GPa, followed by a downstroke to zero pressure and then a second upstroke. The ambient-pressure spectrum is expanded by a factor of three in the region around the TO modes.

onset of the back-transformation to wurtzite. Within a margin of 2 GPa, our wurtzite to rocksalt transition pressure agrees with experimental results reported by other groups [12–16] and with calculated transition pressures [1, 18]. For our experimental conditions (single-crystal starting material, hydrostatic pressure, laser illumination) we could not obtain a single-phase metastable rocksalt modification at ambient pressure.

Figure 2 shows the frequencies of the Raman features of wurtzite ZnO as a function of pressure. Frequencies before and after the phase transition were almost the same within experimental error. Ambient-pressure frequencies, pressure coefficients, and mode Grüneisen parameters are summarized in Table I. The Grüneisen parameters $\gamma = (B_0/\omega_0)(d\omega/dP)$ have been calculated using $B_0 = 143$ GPa for the bulk modulus of ZnO at ambient pressure [14]. The main uncertainty in the γ values arises from the roughly 10% scatter in the experimental values given for the bulk modulus (cf. Ref. [13]).

The assignment of the first-order Raman modes $E_2(\text{low})$, $E_2(\text{high})$, $A_1(\text{TO})$ and $E_1(\text{TO})$ (see Tab. I) is straightforward; their frequencies and pressure coefficients basically agree with data reported in the literature [4–9]. We note that only the scattering by the E_2 and A_1 modes is allowed in the backscattering configuration when the c -axis is oriented parallel to the laser beam. However, partly due to optical reflection effects in the DAC the $E_1(\text{TO})$ mode could also be observed in some of the spectra. We have observed weak or broad features near 213, 331 and 877 cm^{-1} , some of them only during the first upstroke. There is agreement with two-phonon bands reported previously [4–6]. Based on their pressure coefficients, we attribute the features at 213 and 331 cm^{-1} (at ambient pressure) to second-order scattering by the $E_2(\text{low})$ branch around the M point of the Brillouin zone, as suggested by Calleja *et al.* [6], and to the difference mode $E_2(\text{high}) - E_2(\text{low})$, as suggested by

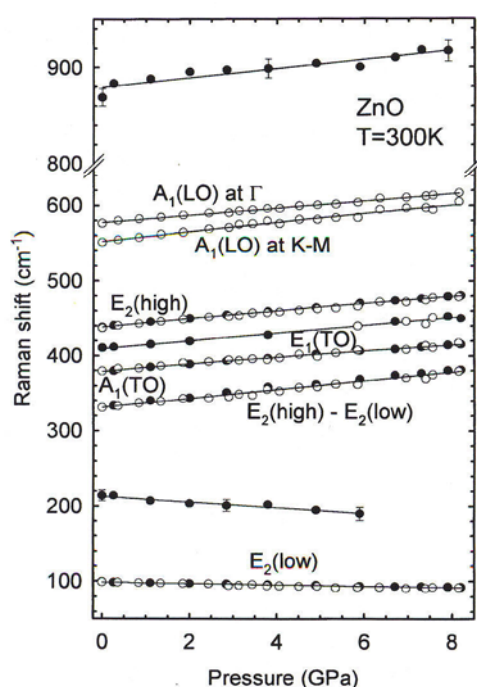


FIGURE 2 Frequencies of Raman features of wurtzite-ZnO as a function of pressure. Solid symbols are for the first upstroke, hollow symbols for the downstroke and second upstroke. Solid lines refer to linear regressions. Error bars are less than or comparable to the size of the symbols, except for broader bands for which the errors are indicated in the figure.

TABLE I Ambient-pressure Frequencies, Pressure Dependencies, and Mode Grüneisen Parameters for Observed Raman Features of Wurtzite-ZnO at 300 K. Pressure Coefficients and Mode Grüneisen Parameters Reported by Other Authors are Listed for Comparison.

Peak/mode	ω_0 cm^{-1}	$d\omega/dP$ $\text{cm}^{-1}/\text{GPa}$	γ	γ
E ₂ (low)	99.5(5)	-0.85(5)	-1.21	-1.75 ^a , -1.80 ^b , -1.69 ^c
Broad band (2nd order)	213(6)	-3.9(6)	-2.58	
E ₂ (high)-E ₂ (low)	331(2)	5.8(2)	2.49	2.45 ^a , 2.48 ^b , 2.28 ^c
A ₁ (TO)	379.0(9)	4.33(8)	1.63	1.7 ^a , 1.33 ^b , 1.65 ^c
E ₁ (TO)	411(3)	5.2(2)	1.80	1.76 ^a , 1.78 ^b
E ₂ (high)	437.9(4)	5.11(7)	1.66	1.62 ^a , 1.61 ^b , 1.65 ^c
See text	540			0.1 ^b
A ₁ (LO) at K-M	550.7(9)	6.0(2)	1.56	
A ₁ (LO) at Γ	576.1(6)	4.75(9)	1.17	1.15 ^a , 0.64 ^b
Broad band (2nd order)	877(7)	4.8(7)	0.78	

^aRef. [7].

^bRef. [8].

^cRef. [9].

Brafman *et al.* [9], respectively. We tentatively attribute the broad feature at 877 cm^{-1} to the overtone of the E₂(high) mode around the ΓM or ΓA direction.

An intense asymmetric Raman feature with intensity maximum near 576 cm^{-1} (ambient pressure) appears after back-transformation to the wurtzite structure. The 576 cm^{-1} peak falls in the frequency range where the A₁(LO) Raman-active modes are expected. The corresponding frequency pressure coefficient is similar to those of the TO modes (see Tab. I). We attribute the 576 cm^{-1} peak to the A₁(LO) mode scattering at the Γ point, consistent with corresponding frequencies reported by other authors [4–6]. The asymmetry, which decreases with increasing pressure, could be caused by a second component centered near 550 cm^{-1} (ambient pressure). In fact, the spectral shape of the asymmetric feature can be well approximated by a superposition of two Gaussians, one for the dominant feature at 576 cm^{-1} and one centered at 550 cm^{-1} . In Table I we list the pressure coefficients of both components.

The low-frequency component seems not to be related to a mode previously observed at 540 cm^{-1} (ambient pressure) [4–6]. At least the two-phonon combinations assigned to the 540 cm^{-1} mode do not agree with the pressure coefficient we observe for the feature near 550 cm^{-1} (see Tab. I). We tent to attribute the low-energy component of the A₁(LO) peak to disorder-induced scattering by LO phonons of non-zero wavevector rather than to a coupled plasmon-phonon mode. This interpretation is consistent with the dispersion of the LO branch in ZnO and the spread of the calculated LO phonon density of states [19], according to which the low-frequency feature arises mainly from LO scattering at zone-edge points (K-M). Within this picture, our results indicate a decrease of the LO branch dispersion with increasing pressure.

The absence of the LO scattering during upstroke can be explained by phonon plasmon coupling. Our crystals had a high residual donor concentration. The interaction of the large density of free carriers with the electromagnetic field associated to the LO phonons leads to a modified line shape and scattering efficiency [3, 20, 21]. The appearance of LO scattering after the back-transformation to the wurtzite phase indicates a decrease of the free electron concentration in the back-transformed samples. It appears that defects created during the wurtzite-rocksalt transition act as electron traps, even at room temperature.

Our experimental data indicate a small *increase* of the LO-TO splitting of the A₁ modes as a function of pressure (see Fig. 3), by an average rate of $0.42(17) \text{ cm}^{-1}/\text{GPa}$ in the pressure range from 0 to 8 GPa. This pressure coefficient is positive, in contrast to the decrease of the

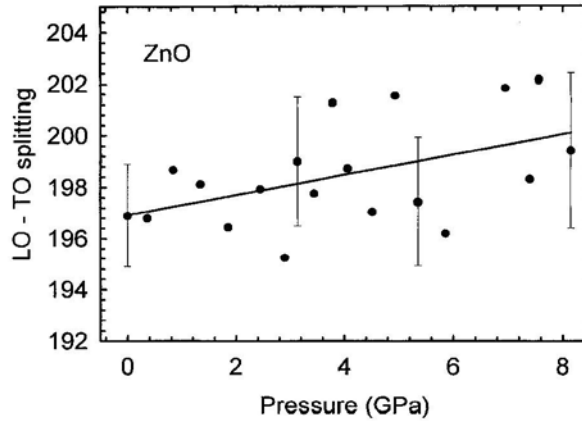


FIGURE 3 Experimental LO-TO splitting in wurtzite ZnO as a function of pressure. The solid line represents a linear regression.

LO-TO splitting occurring in most of the III-V and II-VI compounds [11, 22]. Furthermore, it is comparable to the small changes of the LO-TO splitting in 3C-SiC ($0.85(2) \text{ cm}^{-1}/\text{GPa}$ [23]), 2H-GaN ($0.4(1) \text{ cm}^{-1}/\text{GPa}$ [24]), and 2H-AlN ($0.1(1) \text{ cm}^{-1}/\text{GPa}$ [24]).

The LO-TO splitting of the A_1 modes in wurtzite crystals is related to tensor components of Born's transverse dynamic effective charge e_T^* and of the high-frequency dielectric constant ϵ_∞ [24, 25]. In order to estimate the pressure-induced change of e_T^* in ZnO (2.03 e at ambient conditions), we use $\epsilon_\infty = 3.75$ [26] and a logarithmic volume derivative of $\gamma(\epsilon_\infty) = 0.27$ [27]. With these values we obtain a small change ($1.5(8) \times 10^{-3} \text{ GPa}^{-1}$) of the normalized $e_T^*(P)/e_T^*(0)$ in ZnO with increasing pressure, corresponding to a Grüneisen parameter of about $0.2(1)$. A qualitatively similar behaviour has been reported for SiC [23, 25], GaN, and AlN [24]. The results for ZnO indicate a much smaller change (and opposite in sign) of the bond ionicity under compression if compared to other II-VI and most of the III-V compounds [10, 11].

For the zincblende III-V and II-VI semiconductors it is well known that the shear-type zone-edge TA phonons exhibit negative mode Grüneisen parameters [10]. The wurtzite and zincblende structures differ in the stacking of layers along the cubic $[111]$ direction. The $E_2(\text{low})$ modes of the wurtzite structure are related to the cubic TA(L) modes by folding into the hexagonal zone center. In this way the softening of the $E_2(\text{low})$ mode frequency under pressure can be explained in a way similar to that of the zone-edge TA phonons in zincblende crystals, *i.e.*, in terms of a critical balance between central and non-central elastic forces associated with the stretching and bending of covalent bonds [28]. In this context it should be noted that the shear elastic moduli of ZnO also exhibit a softening under pressure [29], which is typical of the cubic II-VI compounds and is in part responsible for their negative thermal expansion at low temperatures [30].

In summary, we have measured pressure coefficients for Raman mode frequencies of wurtzite ZnO. Our samples initially did not show any detectable $A_1(\text{LO})$ scattering, but developed a strong $A_1(\text{LO})$ feature after pressure cycling through the reversible wurtzite-rocksalt transition (hysteresis 4 GPa). We attribute this behaviour to phonon-plasmon coupling in the as-grown sample and its absence in back-transformed ZnO where defects act as electron traps. We have observed that the LO-TO mode splitting increases slightly in ZnO with increasing pressure, in contrast to most other III-V and II-VI semiconductors. The transverse effective charge in ZnO remains almost constant under pressure. This behaviour appears to

be related to the lack of p -electrons in the anion core [25]. *Ab initio* calculations of the dynamic charge of ZnO at ambient pressure [31] could provide a basis for a more detailed analysis of the observed pressure effects.

Acknowledgements

The authors thank M. Cardona for a critical reading of the manuscript. F. J. M. acknowledges financial support of the European Union through a Marie Curie Fellowship under contract HPMF-CT-1999-00074.

References

- [1] See Ahuja, R., Farst, L., Ericson, O., Willis, J. M. and Johansson, B. (1998). *J. Appl. Phys.*, **83**, 8065 for a collection of references related to applications as well as theoretical work on the phase stability of ZnO under pressure.
- [2] Klein, M. V. (1983). In: Cardona, M. (Ed.), *Light Scattering in Solids*, Vol. I. Springer, Berlin, p. 147.
- [3] Baimanov, B. H., Heinrich, A., Irmer, G., Toporov, V. V. and Ziegler, E. (1983). *Phys. Stat. Sol. (b)*, **119**, 227.
- [4] Damen, T. C., Porto, S. P. S. and Tell, B. (1966). *Phys. Rev.*, **142**, 570.
- [5] Arguello, C. A., Rousseau, D. L. and Porto, S. P. S. (1969). *Phys. Rev.*, **181**, 1351.
- [6] Calleja, J. M. and Cardona, M. (1977). *Phys. Rev. B*, **16**, 3753.
- [7] Minomura, S. (1984). *Mat. Res. Soc. Symp. Proc.*, **22**.
- [8] Sharma, S. K. and Exarhos, G. J. (1997). *Solid State Phenomena*, **55**, 32.
- [9] Brafman, O. and Mitra, S. S. (1971). In: Balkanski, M. (Ed.), *Proceedings 2nd Inter. Conf. on Light Scattering in Solids*, Flammarion, Paris, p. 284 and references therein.
- [10] Weinstein, B. A. and Zallen, R. (1984). In: Cardona, M. and Güntherodt, G. (Eds.), *Light Scattering in Solids*, Vol. IV. Springer, Berlin, p. 463 and references therein.
- [11] Anastassakis, E. and Cardona, M. (1998). In: Suski, T. and Paul, W. (Eds.), *High Pressure in Semiconductor Physics*, Vol. II. Academic, New York, p. 152 and references therein.
- [12] Karzel, H., *et al.* (1996). *Phys. Rev. B*, **53**, 11425.
- [13] Recio, J. M., *et al.* (1998). *Phys. Rev. B*, **58**, 8949.
- [14] Desgreniers, S. (1998). *Phys. Rev. B*, **58**, 14102.
- [15] Kusaba, K., Syono, Y. and Kikegawa, T. (1999). *Proc. Japan Acad. Ser. B*, **75**, 1.
- [16] Decremps, F., Zhang, J. and Liebermann, R. C. (2000). *Europhys. Lett.*, **51**, 268.
- [17] Piermarini, G. J., Block, S., Barnett, J. S. and Forman, R. A. (1975). *J. Appl. Phys.*, **46**, 2774.
- [18] Jaffe, J. E., Snyder, J. A., Lin, Z. and Hess, A. C. (2000). *Phys. Rev. B*, **62**, 1660.
- [19] Kislov, A. N. and Mazurenko, V. G. (1998). *Physics of the Solid State*, **40**, 2009; Camacho, J. (private communication).
- [20] Irmer, G., Toporov, V. V., Baimanov, B. H. and Monecke, J. (1983). *Phys. Stat. Sol. (b)*, **119**, 595.
- [21] Falkovsky, L. A., Knap, W., Chervin, J. C. and Wisniewski, P. (1998). *Phys. Rev. B*, **57**, 11349 and references therein.
- [22] Sanjurjo, J. A., Lopez-Cruz, E., Vogl, P. and Cardona, M. (1983). *Phys. Rev. B*, **28**, 4579 and references therein.
- [23] Olego, D., Cardona, M. and Vogl, P. (1982). *Phys. Rev. B*, **25**, 3878.
- [24] Goñi, A. R., Siegle, H., Syassen, K., Thomsen, C. and Wagner, J.-M. (2001). *Phys. Rev. B*, **64**, 035205.
- [25] Karch, K. and Bechstedt, F. (1996). *Phys. Rev. Lett.*, **77**, 1660.
- [26] Seltemes, E. C. and Swinney, H. L. (1967). *J. Appl. Phys.*, **38**, 2387.
- [27] Vedam, K. and Davis, T. A. (1969). *Phys. Rev.*, **181**, 1196.
- [28] Xu, C. H., Wang, C. Z., Chan, C. T. and Ho, K. M. (1991). *Phys. Rev. B*, **43**, 5024.
- [29] Decremps, F., Zhang, J., Li, B. and Liebermann, R. C. (2001). *Phys. Rev. B*, **63**, 224105.
- [30] Debernardi, A. and Cardona, M. (1996). *Phys. Rev. B*, **54**, 11305.
- [31] Massida, S., Resta, R., Pasternak, M. and Baldereschi, A. (1995). *Phys. Rev. B*, **52**, R16977.